Journal of Molecular Spectroscopy **215,** 275–284 (2002)
doi:10.1006/jmsp.2002.8654

Emission Spectroscopy and *Ab Initio* Calculations for TaN

R. S. Ram,* J. Liévin,† and P. F. Bernath*,‡

*Department of Chemistry, University of Arizona, Tucson, Arizona 85721; †Université Libre de Bruxelles, Laboratoire de Chimie Physique Moléculaire, CP 160/09, Av. F. D. Roosevelt 50, Bruxelles, Belgium; and ‡Department of Chemistry, University of Waterloo, Waterloo, Ontario, Canada N2L 3G1

Received April 10, 2002; in revised form June 26, 2002

The emission spectra of TaN have been investigated in the region 3000–35 000 cm^{-1} using a Fourier transform spectrometer. The spectra were observed in a tantalum hollow-cathode lamp by discharging a mixture of 1.5 Torr of Ne and about 6 mTorr of N_2. In addition to previously known bands, numerous additional bands were observed and assigned to a number of new transitions. The spectroscopic properties of the low-lying electronic states of TaN were also predicted by *ab initio* calculations. A $^1\Sigma^+$ state, with equilibrium constants of $B_e = 0.457\,852\,1(48)$ cm^{-1}, $\alpha_e = 0.002\,235\,9(67)$ cm^{-1}, and $R_e = 1.683\,099\,9(88)$ Å, has been identified as the ground state of TaN based on our experimental observations supported by the *ab initio* results. The first excited state has been identified as the $a^3\Delta_1$ spin component at 2827 cm^{-1} above the ground state. To higher energies, the states become difficult to assign because of their Hund's case (c) behavior and extensive interactions between the spin components of the electronic terms.

INTRODUCTION

Transition-metal-containing molecules are of importance as catalysts in organic and organometallic chemistry (*1–5*) and their spectroscopic studies provide insight into chemical bonding in simple metal-containing systems (*6*). Transition-metal-containing species are also of astrophysical importance (*7–10*). Like many transition metal hydride and oxide molecules, diatomic transition metal nitrides are also potential candidates for discovery in the atmospheres of cool stars. However, precise spectroscopic data for many of these molecules are lacking, making a search in complex stellar spectra difficult.

Over the past several decades, considerable progress has been made toward understanding the electronic structure of transition-metal-containing molecules (*11, 12*). The spectra of these molecules are usually complex because of the presence of a large number of electronic states derived from several close-lying configurations. The presence of open *d*-shells gives rise to states with high spin and large orbital angular momenta, which are split by substantial spin–orbit interactions. Strong spin–orbit interactions limit the validity of the usual Hund's case (a) quantum numbers, and the electronic states have a tendency toward Hund's case (c) coupling. In such cases the subbands of a given electronic transition can be far apart and this creates problems in the electronic assignments. Many of the states and spin components perturb each other and provide impressively complex spectra. TaN is a very good example of such complexity. Although the visible bands of TaN have been known for decades the electronic states remain largely uncharacterized.

The electronic emission spectrum of TaN was first observed in the gas phase in 1975 (*13*) and a rotational analysis of a number of bands was reported in the Ph.D. thesis of Bates. The bands were classified into singlet and triplet systems with strong features near 19 200 and 24 000 cm^{-1}, arising from the two $^1\Pi$ upper states to two low-lying $^1\Sigma$ states. Two bands located near 21 497 cm^{-1} and 23 392 cm^{-1} were analyzed as $^3\Phi_2$–$^3\Delta_1$ and $^3\Phi_3$–$^3\Delta_2$ subbands of a triplet–triplet transition. It was not clear whether the $^3\Delta$ state or one of the two $^1\Sigma$ states was the ground state of TaN. This work was followed by a matrix isolation study of TaN by Bates and Gruen (*14*), who recorded the absorption spectrum of TaN isolated in an argon matrix at 14 K and suggested that a $^1\Sigma^+$ state was most likely the ground state of TaN, because the triplet bands did not appear in absorption. More recently the TaN molecule and its dinitrogen complexes were observed by Zhou and Andrews (*15*) in the reaction of laser-ablated tantalum atoms with nitrogen. The vibrational fundamental of 1058.8 cm^{-1} observed in solid argon (1060 cm^{-1} by Bates and Gruen (*14*)) was empirically corrected to 1070 cm^{-1} for the estimated gas phase value.

In the present work we have recorded the high-resolution emission spectra of TaN in the region 3000–35 000 cm^{-1} using a Fourier transform spectrometer. In addition to the previously known bands, numerous new bands were observed and analyzed. *Ab initio* calculations have also been performed to predict the spectroscopic properties of the low-lying electronic states. The analysis of the observed bands and their electronic assignments based on our *ab initio* calculations will be presented in this paper. The ground state of TaN has been identified as a $^1\Sigma^+$ state based on our experimental observations and our *ab initio* results.

AB INITIO CALCULATIONS

Large-scale *ab initio* calculations have been performed on the valence electronic states of TaN lying less than 25 000 cm^{-1}

Supplementary data for this article may be found on the journal home page.

0022-2852/02 $35.00

above the ground state. Fourteen electronic states, corresponding to seven singlet, five triplet, and two quintet states, are predicted in this range. Their potential energy curves and the corresponding spectroscopic properties have been calculated using a CASSCF/CMRCI computational approach adopted with success in a series of studies on transition-metal-containing diatomic molecules such as nitrides (*16–18*), oxides (*19*), and chlorides (*20, 21*). In brief, the procedure consists of a preliminary optimization of the molecular orbitals by state-averaged full-valence CASSCF calculations (*22*), followed by an internally contracted multireference configuration interaction (CMRCI) calculation (*23*) correlating all valence electrons. Davidson's correction (*24*) for four-particle unlinked clusters is added to the CMRCI energies. Quasi-relativistic Wood–Boring pseudopotentials are used on both atoms. They describe the 60 and the 2 core electrons of the Ta and N atoms, respectively (*25, 26*). The valence double zeta basis sets (*25, 26*) consistent with the core potentials were augmented by a single Gaussian polarization orbital on each atom (an f-type function with an exponent of 0.8 on Ta and a d-type function with an exponent of 0.8 on N). The active valence orbital space is defined by the four σ, two π, and one δ molecular orbital arising from the $5d$ and $6s$ orbitals of Ta and the $2s$ and $2p$ orbitals of N. The two σ and the π orbitals correlating to the $5s$ and $5p$ orbitals of Ta, not involved in the core potential, are explicitly included in the variational procedure, but are kept doubly occupied in all wave functions. The size of the CASSCF (CMRCI) wave functions range from 3000 to 7500 (290 000 to 600 000) configuration state functions (C_{2v} symmetry) depending on the space and spin symmetries of the considered electronic states. All calculations were performed with the MOLPRO package (*27*) running on the Compaq alpha servers of the ULB/VUB computer center.

ELECTRONIC STRUCTURE OF TaN FROM *AB INITIO* CALCULATIONS

The potential energy curves of the 14 low-lying electronic states of TaN have been obtained from CMRCI calculations performed at a set of internuclear distances ranging between 1.5 and 2.2 Å and separated by 0.05 Å. Figure 1 shows the potential curves of the singlet, triplet, and quintet spin manifolds represented in separate panels. The energy scale is relative to the minimum energy of the $X^1\Sigma^+$ ground electronic state. The spectroscopic properties calculated from all these states are given in Table 1, where the following properties are reported: the equilibrium internuclear distances R_e, the harmonic frequencies at equilibrium ω_e, and the term energies T_0, corrected for the zero point energy contribution calculated within the harmonic approximation.

The analysis of the corresponding wave functions is provided in Tables 2 and 3 and the electronic structure of TaN is illustrated in Figs. 2 and 3. Table 2 gives a list of 23 configurations, labeled from (A) to (W), which have a weight greater than or equal to 2% in the CMRCI wave functions. The configuration weights

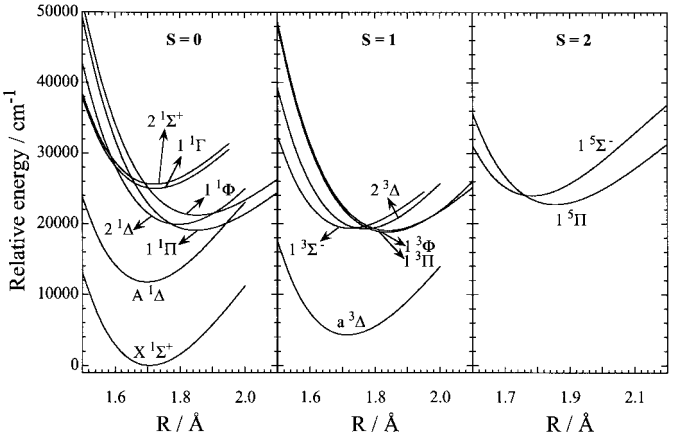

FIG. 1. The low-lying potential-energy curves of TaN in the singlet, triplet, and quintet spin systems from CMRCI calculations.

are calculated as the sum of the squares of the CI coefficients of CSFs belonging to the corresponding electronic configurations. The weights are reported in Table 3 for all 14 states. Table 2 characterizes the electronic configurations in terms of electron promotions with respect to the ground configuration, which is predicted by our calculations to be $1\sigma^2 2\sigma^2 1\pi^4 3\sigma^2$ (configuration (A)), leading to the $X^1\Sigma^+$ ground state. Note that the numbering of the molecular orbitals refers to the valence orbitals only, which assumes a core of 70 electrons common to all configurations.

TABLE 1

Spectroscopic Properties of the Low-Lying Electronic States of TaN from CMRCI Calculations (See Fig. 1) Experimental Values Are Given in Parentheses

Multiplicity	State	T_0 (cm^{-1})	R (Å)	ω_e (cm^{-1})
1	$X^1\Sigma^+$	0	1.706 (1.6831)[a]	1049 (1070)[b]
	$A^1\Delta$	11 727	1.698	1053
	$1^1\Pi$	18 944	1.849	824
	$2^1\Delta$	19 790	1.794	900
	$1^1\Phi$	21 052	1.852	817
	$1^1\Gamma$	24 899	1.723	924
	$2^1\Sigma^+$	25 512	1.72	949
3	$a^3\Delta$	4276 (2827.2917)[c]	1.714 (1.6915)[c]	999 —
	$1^3\Pi$	18 732	1.837	859
	$1^3\Phi$	18 951	1.841	848
	$2^3\Delta$	19 230	1.767	950
	$1^3\Sigma^-$	19 298	1.724	919
5	$1^5\Pi$	22 603	1.854	814
	$1^5\Sigma^-$	23 870	1.783	894

[a] This work.

[b] Estimated gas phase value, empirically corrected from an argon matrix spectrum (*15*).

[c] Values are for the $a^3\Delta_1$ spin component.

TABLE 2

Electronic Configurations Describing the Electronic States of TaN below 25 000 cm^{-1} (See Table 3), Defined by the Electron Promotions with Respect to the Ground Configuration $1\sigma^2 2\sigma^2 1\pi^4 3\sigma^2$, Referred to as Configuration (A)

Labels	Configurations[a]	Number of excitations
(B)	$3\sigma \rightarrow 1\delta$	1
(C)	$1\pi \rightarrow 1\delta$	1
(D)	$2\sigma \rightarrow 1\delta$	1
(E)	$3\sigma^2 \rightarrow 1\delta^2$	2
(F)	$1\pi 3\sigma \rightarrow 1\delta^2$	2
(G)	$2\sigma 3\sigma \rightarrow 1\delta^2$	2
(H)	$1\pi^2 \rightarrow 2\pi^2$	2
(I)	$1\pi^2 \rightarrow 1\delta 2\pi$	2
(J)	$2\sigma 3\sigma \rightarrow 1\delta 4\sigma$	2
(K)	$2\sigma 1\pi \rightarrow 1\delta 2\pi$	2
(L)	$2\sigma 1\pi \rightarrow 2\pi 4\sigma$	2
(M)	$1\pi^2 3\sigma \rightarrow 1\delta 2\pi^2$	3
(N)	$2\sigma 3\sigma^2 \rightarrow 1\delta^3$	3
(O)	$2\sigma 1\pi^2 \rightarrow 1\delta 2\pi^2$	3
(P)	$1\pi^3 \rightarrow 1\delta 2\pi^2$	3
(Q)	$2\sigma 1\pi 3\sigma \rightarrow 1\delta 2\pi 4\sigma$	3
(R)	$2\sigma 1\pi 3\sigma \rightarrow 1\delta^2 2\pi$	3
(S)	$1\pi^2 3\sigma^2 \rightarrow 1\delta^2 2\pi^2$	4
(T)	$1\pi^3 3\sigma \rightarrow 1\delta^2 2\pi^2$	4
(U)	$2\sigma 1\pi 3\sigma^2 \rightarrow 1\delta^2 2\pi 4\sigma$	4
(V)	$2\sigma 1\pi^2 3\sigma \rightarrow 1\delta^2 2\pi^2$	4
(W)	$2\sigma 1\pi^2 3\sigma \rightarrow 1\delta^2 2\pi 4\sigma$	4

[a] Configurations (A) to (G) are the main configurations in the low-lying states (weights greater than 70% in the corresponding wave functions). Configurations (H) to (W) are secondary configurations (see Table 3).

TABLE 3

Analysis of the CMRCI Wave Functions of TaN in Terms of Electronic Configurations (See Table 2 for the Configuration Labeling)

Electronic state	Weight[a]
$X^1\Sigma^+$	77% (A) + 6% (E) + 4% (H) + 2% (L)
$A^1\Delta$	82% (B) + 4% (M) + 3% (Q)
$1^1\Pi$	77% (C) + 3% (I) + 3% (P)
$2^1\Delta$	67% (D) + 4% (K) + 4% (J) + 3% (O)
$1^1\Phi$	76% (C) + 2% (I) + 3% (P)
$1^1\Gamma$	85% (E) + 3% (R)
$2^1\Sigma^+$	74% (E) + 6% (A) + 3% (S) + 2% (U)
$a^3\Delta$	82% (B) + 4% (M) + 2% (Q)
$1^3\Pi$	76% (C) + 4% (F) + 2% (P)
$1^3\Phi$	80% (C) + 3% (P)
$2^3\Delta$	79% (D) + 3% (O) + 2% (N)
$1^3\Sigma^-$	84% (E) + 4% (S) + 3% (R)
$1^5\Pi$	85% (F) + 3% (T) + 2% (W)
$1^5\Sigma^-$	85% (G) + 4% (V)

[a] Weights (in percent) are obtained from the square of the corresponding configuration interaction coefficients; weights lower than 2% are not reported.

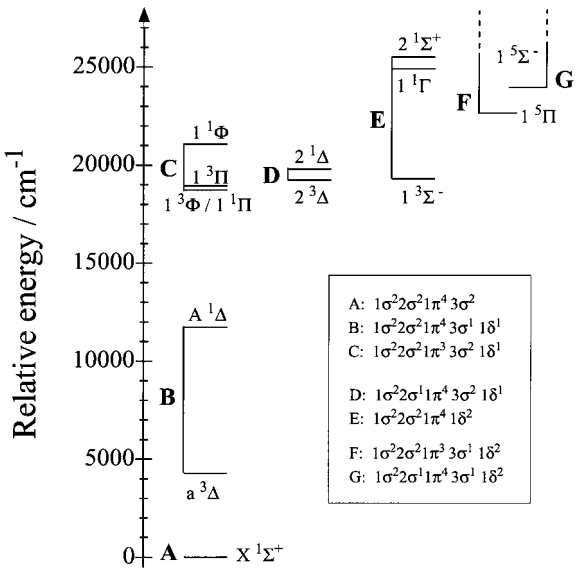

FIG. 2. The electrostatic splitting of the low-lying electronic configurations of TaN from CMRCI calculations.

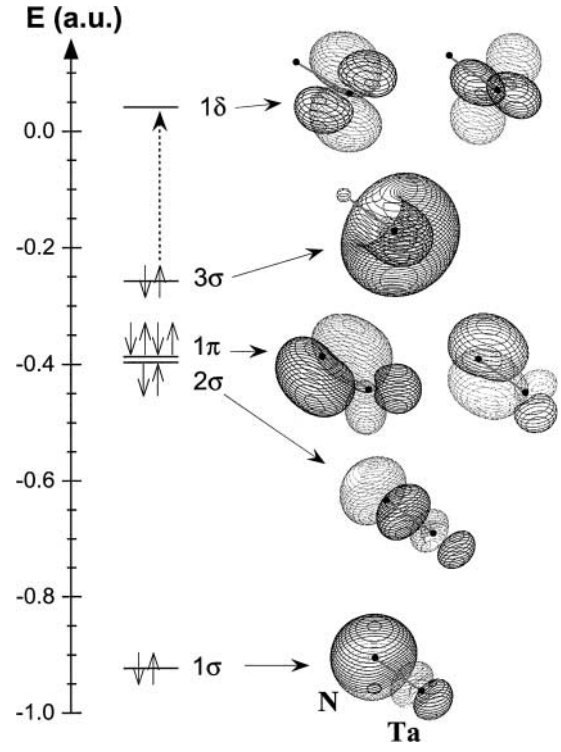

FIG. 3. The molecular orbital diagram for TaN, from full valence CASSCF calculations performed on the $X^1\Sigma^+$ state (1σ, 2σ, 1π, and 3σ) and on the $1^3\Delta$ state (1δ). The orbital shapes are obtained for a contour value of the wave function fixed to 0.025. Solid and dotted lines correspond to positive and negative values of the wave function, respectively. The orbital filling corresponds to the ground electronic configuration (A) and the dashed arrow indicates the single excitation.

All calculated states can be described mainly from the set of configurations (A) to (G) having a weight larger than 70% in the corresponding wave functions. All secondary configurations (H) to (W) have small weights (maximum of 6%). This means that no dramatic configuration mixing and no avoided crossings are encountered for the considered states. The complexity of the electronic structure of TaN comes, however, from the large number of states (*11*) within the range 18 000–25 000 cm^{-1}. One sees from Fig. 1 that only the three low-lying states are well separated. This is better illustrated in Fig. 2, where the electrostatic splitting of the major configurations (A) to (G) is represented. This splitting can be explained from the molecular orbital diagram given in Fig. 3. Energies and orbital shapes have been obtained from CASSCF calculations performed on the lowest electronic states in which these orbitals are actually occupied, i.e., the ground state for orbitals 1σ, 2σ, 1π, and 3σ and the $1^3\Delta$ state for orbital 1δ. The orbital energy pattern of Fig. 3 suggests that the low-lying electronic states should arise from electronic excitations from the close-lying 2σ, 1π, and 3σ orbitals to the orbital 1δ. The virtual 2π and 4σ valence orbitals, not reproduced on the diagram, are lying at higher energies (0.2 and 0.34 a.u. from 1δ, respectively) and are not expected to contribute significantly to the electronic structure. This is actually confirmed by the calculations, as shown in Fig. 2. The low level of mixing between major and secondary configurations in the wave functions (see Table 3) is another consequence of this orbital energy distribution, in particular from the quasi degeneracy of the $(2\sigma, 1\pi, 3\sigma)$ set of orbitals. As can be seen from Table 2, configurations (H) to (W) involve multiply excited configurations (2 to 4 electron promotions) with weights of the same order of magnitude. A large energy gap is therefore expected between (A–G) and (H–W). As a proof, we have calculated the vertical term energies of some excited states lying above the 14 states considered. This calculation has been performed at the CASSCF level of theory and we found the values of 29 000, 32 570, 34 973, 35 801, 37 067, 39 760, 39 861, 40 083, 42 043, and 43 022 cm^{-1} for the $2^3\Pi$, $1^1\Sigma^-$, $2^3\Phi$, $1^5\Delta$, $2^1\Phi$, $2^1\Pi$, $1^5\Gamma$, $1^5\Phi$, $1^5\Sigma^+$, and $2^3\Sigma^+$ states, respectively. A comparison of the CASSCF values with the corresponding CMRCI ones (see Table 1) for the 14 states below 25 000 cm^{-1} shows that the former values are overestimated by an amount varying between 1000 and 5000 cm^{-1} depending on the states considered. This gives an order of magnitude for the dynamical correlation energy contributions introduced by the large scale CMRCI approach. One can thus conclude that except for the $2^3\Pi$ state, which could be close to the 25 000 cm^{-1} limit, all other states are predicted to be significantly higher.

Orbital shapes, obtained from the program Molden (*28*) and drawn in Fig. 3, allow a qualitative description of the electronic structure, which can be summarized as follows:

—1σ is a bonding combination of $5p_z$(Ta) with $2s$(N), with a minor contribution by $5d_0$(Ta),

—2σ is a bonding combination of $5d_0$(Ta) with $2p_z$(N), with a minor contribution by $6s$(Ta),

—1π is a bonding combination of $5d_{\pm1}$(Ta) with $2p_{\pm1}$(N),

—3σ is a nearly pure orbital on Ta in which $5d_0$ and $6s$ are mixed,

—1δ corresponds to the $5d_{\pm2}$ orbital of Ta,

—2π and 4σ are the antibonding counterparts of orbitals 1π and 2σ, respectively.

Complementary information is given by the Mulliken atomic population analysis of the CASSCF wave functions, from which one can quantify the number of electrons in s-, p-, and d-type atomic orbitals on both atoms and deduce the degree of ionicity, defined as $Ta^{+\delta}N^{-\delta}$. One obtains, for the three low-lying states:

$$X^1\Sigma^+ : s^{1.60}p^{0.25}d^{2.90}\ (\mathrm{Ta})\ s^{1.84}p^{3.41}\ (\mathrm{N});\ \delta = 0.25$$

$$a^3\Delta : s^{0.92}p^{0.27}d^{3.50}\ (\mathrm{Ta})\ s^{1.83}p^{3.47}\ (\mathrm{N});\ \delta = 0.30$$

$$A^1\Delta : s^{1.33}p^{0.24}d^{3.16}\ (\mathrm{Ta})\ s^{1.81}p^{3.46}\ (\mathrm{N});\ \delta = 0.27$$

EXPERIMENTAL

The TaN molecule was made in a tantalum hollow-cathode lamp which was prepared by tightly inserting a solid tantalum metal rod into a 10-mm hole in a copper block. The metal was then bored through to provide a 1-mm-thick layer of Ta metal on the inside wall of the copper hole. The lamp was operated with a current at 560 V and 400 mA with a slow flow of a mixture of 1.5 Torr of Ne and about 6 mTorr of N_2 through the lamp. The emission from the lamp was observed with the 1-m Fourier transform spectrometer associated with the McMath–Pierce Solar Telescope of the National Solar Observatory.

The spectrum in the region 3000–10 000 cm^{-1} were recorded using a CaF_2 beam splitter, liquid-nitrogen-cooled InSb detectors, and a green glass filter by coadding 15 scans in 2 h of integration at a resolution of 0.02 cm^{-1}. For the region 9500–35 000 cm^{-1} the spectrometer was equipped with a UV beam splitter and midrange diode detectors. The spectra from 9500 to 19 500 cm^{-1} were recorded using a GG 495 filter by co-adding 15 scans in about 3 h and 15 min of integration and the spectra in the region 19 000–35 000 cm^{-1} were recorded using a $CuSO_4$ filter by co-adding 20 scans in about 2 h 20 min of integration. For both regions the spectrometer resolution was set at 0.02 cm^{-1}. In addition to the TaN bands, the observed spectra also contained Ta and Ne atomic lines and also some N_2 molecular bands.

The line positions were extracted from the observed spectra using a data reduction program called PC-DECOMP developed by J. Brault. The peak positions were determined by fitting a Voigt line shape function to each spectral feature. The spectra were calibrated using the measurements of Ne atomic lines made by Palmer and Engleman (*29*). The absolute accuracy of the wavenumber scale is expected to be of the order of ±0.003 cm^{-1}. The TaN lines in the stronger bands appear with a maximum signal-to-noise ratio of about 20 and have a typical line width of about 0.05 cm^{-1}. The precision of measurements of strong and unblended TaN lines is expected to be better than ±0.003 cm^{-1}.

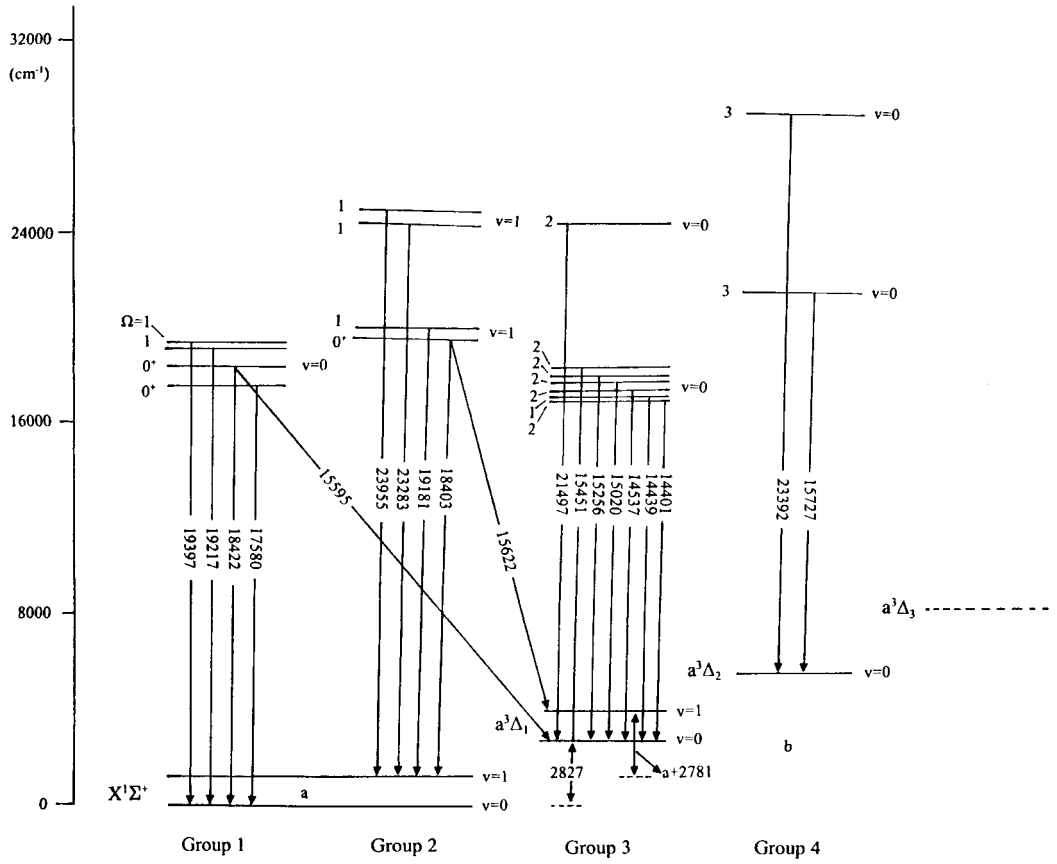

FIG. 4. An energy-level diagram of the observed transitions of TaN.

The precision of measurements for the weaker and overlapped lines is limited to ± 0.005 cm^{-1}.

OBSERVATIONS AND ANALYSIS

In addition to the known bands from the previous gas phase study (*13*), a number of additional bands have been observed over the entire region extending from 10 000 to 25 000 cm^{-1}. The lower (<10 000 cm^{-1}) and the higher wavenumber (>25 000 cm^{-1}) regions are overlapped by strong N_2 bands and no definite heads attributable to TaN were identified. The observed bands have been classified into four groups, as shown in the schematic energy level diagram provided in Fig. 4. The lower states of the four group of bands have been assigned as the $X^1\Sigma^+ v = 0, X^1\Sigma^+ v = 1, a^3\Delta_1 v = 0$ and $a^3\Delta_2 v = 0$. These assignments are supported by our *ab initio* calculations. There are a few additional isolated bands which have been rotationally analyzed but do not have rotational constants common to the bands falling in the four groups. Several badly perturbed bands still remain to be rotationally analyzed.

The branches in different bands were sorted using a color Loomis–Wood program running on a PC computer. This program was very helpful in identifying the lines particularly in the weaker and overlapped bands. The molecular constants were determined by fitting the observed line positions with the customary energy level expressions:

(for $^1\Sigma^+$ and higher Ω states)

$$F_v(J) = T_v + B_v J(J+1) - D_v[J(J+1)]^2 + H_v[J(J+1)]^3 + L_v[J(J+1)]^4. \quad [1]$$

(for $^1\Pi$ states)

$$F_v(J) = T_v + B_v J(J+1) - D_v[J(J+1)]^2 + H_v[J(J+1)]^3 + L_v[J(J+1)]^4 \pm 1/2\{q_v J(J+1) + q_{D_v}(J(J+1))^2 + q_{H_v}(J(J+1))^3 + q_{L_v}(J(J+1))^4\}. \quad [2]$$

The blended and perturbed lines were given a reduced weighting and badly overlapped lines were excluded in order to improve the standard deviation of the fit. Since most of the excited states are affected by interactions with close-lying states, several higher order rotational and Λ-doubling constants were required. In the final fits, the lower state combination differences from the strong and relatively unperturbed bands of that group were also included with higher weights. The line positions in the bands may be obtained from the authors upon request or from the supplementary data. The molecular constants obtained from the final fits are provided in Table 4.

TABLE 4
Spectroscopic Constants[a] (in cm^{-1}) for the Observed States of TaN

(A) Constants for the $X^1\Sigma^+$, $a^3\Delta_1$ and $a^3\Delta_2$ states

	$X^1\Sigma^+$		$a^3\Delta_1$		$a^3\Delta_2$
Constants	$v=0$	$v=1$	$v=0$	$v=1$	$v=0$
T_v	0.0	a	2827.2917(24)	$a+2780.6802(23)$	b
B_v	0.456 734 1(34)	0.454 498 2(58)	0.452 160 7(31)	0.449 833 7(53)	0.453 324 8(70)
$10^7 \times D_v$	3.3508(63)	3.325(12)	3.5483(54)	3.527(11)	3.499(12)

(B) Constants for the excited states of bands in group 1

Constants	$[17\,580]\Omega=0^+$	$[18\,422]\Omega=0^+$	$[19\,217]\Omega=1$	$[19\,397]\Omega=1$
T_v	17 580.4995(21)	18 422.4321(26)	19 217.4310(22)	19 397.3799(15)
B_v	0.436 939 1(62)	0.430 293 0(44)	0.43 441 5(10)	0.423 486 5(82)
$10^6 \times D_v$	−0.6691(40)	1.1166(20)	2.534(12)	−1.201(11)
$10^{10} \times H_v$	−1.237(11)	1.6810(46)	−1.253(56)	2.006(50)
$10^{14} \times L_v$	0.5187(95)	−0.9333(35)	2.499(81)	−2.634(13)
$10^4 \times q_v$	—	—	2.799(27)	2.148(95)
$10^7 \times q_{D_v}$	—	—	−0.319(10)	−1.30(19)
$10^{10} \times q_{H_v}$	—	—	—	1.272(92)

(C) Constants for the excited states of bands in group 2

Constants	$[a+18\,403]\Omega=0^+$	$[a+19\,181]\Omega=1$	$[a+23\,283]\Omega=1$	$[a+23\,955]\Omega=1$
T_v	$a+18\,402.9738(25)$	$a+19\,180.6447(33)$	$a+23\,282.8527(70)$	$a+23\,954.91(14)$
B_v	0.423 471 5(85)	0.44 228 7(42)	0.41 266 6(43)	0.37 264(57)
$10^5 \times D_v$	−0.15 676(55)	0.327(17)	−1.8085(83)	−4.352(87)
$10^8 \times H_v$	−0.00673(16)	0.436(26)	−0.6448(62)	−1.797(57)
$10^{12} \times L_v$	0.00110(16)	−2.78(14)	0.883(16)	2.55(13)
$10^3 \times q_v$	—	0.990(46)	0.612(16)	1.387(31)
$10^6 \times q_{D_v}$	—	−4.19(26)	−0.647(30)	−1.826(59)
$10^9 \times q_{H_v}$	—	8.25(47)	0.226(13)	0.631(27)
$10^{12} \times q_{L_v}$	—	5.38(27)	—	—

(D) Constants for the excited states of bands in group 3

Constants	$[17\,228]\Omega=2$	$[17\,266]\Omega=1$	$[17\,364]\Omega=2$	$[17\,847]\Omega=2$
T_v	17 228.0784(32)	17 266.0048(30)	17 363.5767(31)	17 846.8085(27)
B_v	0.399 824 2(57)	0.426 213 3(49)	0.407 726 5(78)	0.428 296 1(39)
$10^6 \times D_v$	0.5165(31)	0.3980(25)	1.6543(69)	1.5166(16)
$10^{10} \times H_v$	0.0782(57)	−0.0651(46)	1.193(18)	−0.5770(35)
$10^{15} \times L_v$	—	—	—	4.600(25)
$10^5 \times q_v$	—	2.72(37)	—	—
$10^8 \times q_{D_v}$	—	−1.22(35)	—	—
$10^{11} \times q_{H_v}$	—	1.223(77)	—	—

Constants	$[18\,083]\Omega=2$	$[18\,278]\Omega=2$	$[24\,325]\Omega=2$
T_v	18 083.2185(29)	18 277.9667(29)	24 324.524(25)
B_v	0.427 129 6(46)	0.413 180 2(49)	0.44 621(19)
$10^6 \times D_v$	1.6674(24)	−0.5868(30)	3.48(47)
$10^9 \times H_v$	0.02871(61)	0.05552(81)	4.28(49)
$10^{12} \times L_v$	0.005187(51)	0.005474(74)	−3.82(18)

[a] Values in parentheses are one standard deviation in the last digits quoted.

TABLE 4—*Continued*

(E) Constants for the excited states of bands in group 4

Constants	$[b+15\,727]\Omega=3$	$[b+23\,392]\Omega=3$
T_v	$b+15\,727.4062(33)$	23 391.8919(67)
B_v	0.44 038 6(15)	0.44 771 1(77)
$10^6\times D_v$	0.113(18)	3.77(27)
$10^9\times H_v$	0.0880(87)	4.75(37)
$10^{12}\times L_v$	−0.0285(14)	−4.29(17)

(F) Constants for other bands with uncertain electronic assignments

Constants	$\Delta\Omega=1$	$\Delta\Omega=1$	$\Delta\Omega=1$	$\Delta\Omega=1$
T_{vv}	15 420.1152(29)	21 003.7497(30)	23 163.9827(74)	18 732.7754(48)
B'_v	0.42 959 8(26)	0.42 540 6(26)	0.42 104 1(62)	0.42 118 6(99)
$10^6\times D'_v$	−0.4379(86)	0.5291(91)	0.410(28)	2.201(86)
$10^{10}\times H'_v$	−0.955(11)	−1.420(16)	—	4.65(26)
$10^{14}\times L'_v$	—	—	—	−7.03(24)
$10^4\times q'_v$	—	—	—	8.164(99)
$10^7\times q'_{D_v}$	—	—	—	−3.85(13)
$10^{11}\times$	—	—	—	8.55(42)
B''_v	0.44 512 7(25)	0.44 512 7(25)	0.44 862 6(63)	0.45 072 5(96)
$10^7\times D''_v$	3.409(62)	3.409(62)	4.42(29)	9.69(81)
$10^{10}\times$	—	—	—	1.78(21)

1. The $X^1\Sigma^+$ Ground State

The bands with the origins near 17 580, 18 422, 19 217, and 19 397 cm^{-1} have a common lower state. Of these, the bands located near 17 580 and 18 422 cm^{-1} have single R and P branches and are, therefore, $\Delta\Omega=0$ transitions consistent with a $^1\Sigma^+$–$^1\Sigma^+$ ($\Omega=0^+\rightarrow 0^+$) assignment. The bands located near 19 217 and 19 397 cm^{-1} have single P, Q and R branches with combination defects indicating that they involve $^1\Pi$–$^1\Sigma^+$ ($\Omega=1\rightarrow 0^+$) type of transitions. The $^1\Sigma^+$–$^1\Sigma^+$ transitions are free from local perturbations although they are affected by global interactions. The lines up to $R(75)$, $P(76)$ and $R(63)$, $P(62)$ have been identified in the bands 17 580 and 18 422 cm^{-1}, respectively. The band 19 397-cm^{-1}, on the other hand, is involved in a local perturbation in the excited state in which the e-parity levels are perturbed near $J'=43$, as evident from the R and P branches. The f-levels of the excited state are not perturbed. The band 19 217 cm^{-1} is also perturbed locally near $J'=38$ in the e-parity levels. Most of the lines in the perturbation range were deweighted. A part of the 19 397 cm^{-1} band near the R-head is presented in Fig. 5. The need for higher order constants in all the excited states reflects the presence of global interactions. The common $^1\Sigma^+$ lower state of this group of transitions has been identified as the $v=0$ vibrational level of the ground state of TaN with $B_0=0.456\,734\,1(34)$ cm^{-1}. This ground state assignment is supported by our *ab initio* calculations described in preceding sections which predict a $^1\Sigma^+$ ground state for TaN arising from the $1\sigma^2 2\sigma^2 1\pi^4 3\sigma^2$ electronic configuration.

In the second group the bands with origins near 18 403, 19 181, 23 283, and 23 955 cm^{-1} have a common lower state with a rotational constant of $B=0.454\,498\,2(58)$ cm^{-1}. This state has been assigned as the $v=1$ vibrational level of the ground state. These assignments provide $B_e=0.457\,852\,1(48)$ cm^{-1} and $\alpha_e=0.002\,235\,9(67)$ cm^{-1} for the $X^1\Sigma^+$ state. The predicted (*15*) vibrational interval is about 1070 cm^{-1} in the ground state. Unfortunately we could not find any 0–1 bands at this interval from the 0–0 bands of the four transitions of the first group. We are, therefore, unable to determine the gas phase vibrational interval for the ground state.

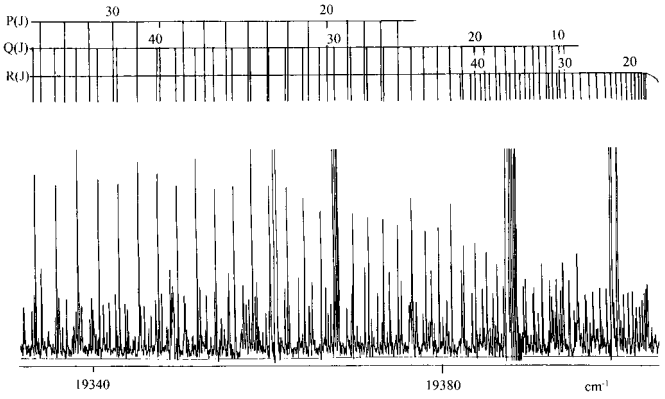

FIG. 5. A portion of the ($\Omega=1$)–$X^1\Sigma^+$ (19 397 cm^{-1}) transition of TaN near the R head.

2. The $a^3\Delta_1$ Spin Component of the First Excited State

Eight bands with origins near 21 498, 15 595, 15 451, 15 256, 15 020, 14 537, 14 439, and 14 401 cm^{-1} have been collected in group 3 (Fig. 4). These bands have a common lower state which has been assigned as the $v = 0$ vibrational level of the $^3\Delta_1$ spin component of the first excited $a^3\Delta$ state. In the previous work on TaN only one band with origin near 21 498 cm^{-1} was observed involving this lower state. In the present work seven additional bands lying to lower wavenumbers of the region covered by Bates (*13*) have been observed and analyzed. The observation of a band located near 15 595 cm^{-1} having a common excited state ($B' = 0.430\,3\ cm^{-1}$, $D' = 1.12 \times 10^{-6}\ cm^{-1}$) with a band at 18 422 cm^{-1} in group 1 has provided a major breakthrough in the assignment of the low-lying states of TaN. The 18 422 cm^{-1} state has been assigned as an $\Omega = 0^+$ state. The band 15 595 cm^{-1} of group 3 has P, Q, and R branches with no combination defects, which supports the 0^+–$^3\Delta_1$ assignment for this transition, with no Ω-doubling in the $^3\Delta_1$ state. The observation of this intercombination transition enables us to combine the bands belonging to groups 1 and 3. The combined fit places the $^3\Delta_1$ $v = 0$ state at 2827 cm^{-1} above the ground state. The 14 401, 14 537, 15 020, 15 256, 15 451, and 21 498 cm^{-1} bands have P, Q, and R branches with no combination defects, suggesting that high Ω states are involved in these transitions. Ω values of 2 have been assigned to the excited states of these transitions, although 0^+ and 0^- states are also possible. Note that any 0^- states would not connect to the $X^1\Sigma^+$ ground state. First lines were not observed, so we cannot confirm these Ω values. A part of the ($\Omega = 2$)–$a^3\Delta_1$ band at 15 020 cm^{-1} is presented in Fig. 6. This band is free from perturbations and lines up to $R(64)$, $P(65)$, and $Q(86)$ have been identified. A $\Delta\Omega = 0$ band at 14 439 cm^{-1} with two R and two P branches has been assigned as $a^3\Delta_1$ $-^3\Delta_1$ transition, with Ω-doubling in the excited $\Omega = 1$ state. The lower $a^3\Delta_1$ state of this group has a rotational constant of $B_0 = 0.452\,160\,7(31)\ cm^{-1}$.

Another band located near 15 622 cm^{-1}, with P, Q, and R branches with no combination defects, has its upper state in common with the 18 403 cm^{-1} band of group 2. When we combine the band at 15 622 cm^{-1} with the other bands belonging to the second group of bands, we find that the lower state of the 15 622 cm^{-1} band is located at 2781 cm^{-1} above the $v = 1$ vibrational level of the ground $X^1\Sigma^+$ state. This value is very similar to the ($^3\Delta_1$, $v = 0$)–($X^1\Sigma^+$, $v = 0$) separation of 2827 cm^{-1}. We have assigned this lower state as the $v = 1$ vibrational level of the $a^3\Delta_1$ state. The rotational constant of $B_1 = 0.449\,833\,7(53)\ cm^{-1}$ for this lower state provides $B_e = 0.453\,324\,2(43)\ cm^{-1}$ and $\alpha_e = 0.002\,327\,0(43)\ cm^{-1}$ for the $a^3\Delta_1$ state.

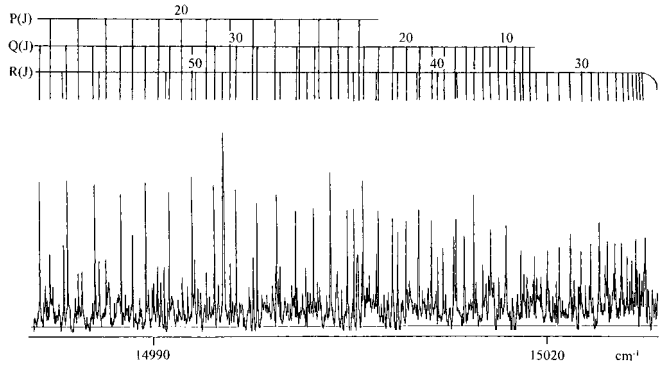

FIG. 6. A portion of the ($\Omega = 2$)–$a^3\Delta_1$ (15 020 cm^{-1}) transition of TaN near the R head.

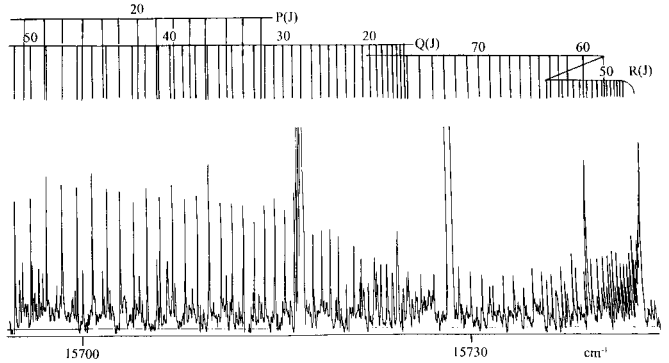

FIG. 7. A portion of the ($\Omega = 3$)–$a^3\Delta_2$ (15 727 cm^{-1}) transition of TaN near the R head.

3. The $a^3\Delta_2$ Spin Component of the First Excited State

The two bands with origins near 15 727 and 23 392 cm^{-1} have been assigned as involving the $^3\Delta_2$ $v = 0$ spin component of the $a^3\Delta$ state. The 23 392 cm^{-1} band was also observed previously by Bates (*13*). Both of the bands in this group have P, Q, and R branches with no combination defects. The rotational lines in the 23 392 cm^{-1} band could not be identified beyond $J' = 37$ because of strong perturbations at higher J values. A part of the new band at 15 727 cm^{-1} has been provided in Fig. 7. This band is affected by a local perturbation near $J' = 59$, which can be noticed in the R branch in Fig. 7. Lines up to $R(76)$, $P(65)$, and $Q(77)$ were identified in this band in spite of perturbations. The third $^3\Delta_3$ spin component of the $a^3\Delta$ state has not been assigned.

4. Other Isolated and Unassigned Bands

There are several isolated bands which have been rotationally analyzed but whose electronic assignment remains uncertain. For example, a band near 23 164 has P, Q, and R branches with no combination defects. This band is free from perturbations and has a lower state constant of 0.4486 cm^{-1}. The lower state of this band may well be the $v = 2$ level of the $a^3\Delta_2$ spin component but the $v = 1$ vibrational level is yet to be identified. We have also found two additional bands near 15 420 and 21 004 cm^{-1} with no combination defects and a common lower state with a rotational constant of $B = 0.4451\ cm^{-1}$. So far we have no assignment of this lower state. Another weak band at 18 733 cm^{-1} has P, Q,

and R branches with combination defects indicating a $\Delta\Omega = 1$ transition with one state having an $\Omega = 0^+$ state. The electronic assignment of this band also remains uncertain. There are several other bands near 19 018, 21 239, 21 380, 23 620, 24 220, and 25 502 cm^{-1} which remain unanalyzed because of strong perturbations or their weaker intensity. Also, there are numerous strong TaN molecular lines in the region 21 350–21 600 cm^{-1} with no pronounced heads, which may belong to one or more additional bands. Some of these bands may involve the $^3\Delta_3$ spin component of the $a^3\Delta$ state.

DISCUSSION

As has been mentioned by Bates (*13*) and also observed in the present work, the visible spectrum of TaN is very complex because of frequent perturbations which results in incomplete analysis of the bands. This has made the electronic assignment of the observed bands a challenging job. In our work we have been able to analyze a number of new bands which are relatively less affected by perturbations. The effects of interactions can clearly be seen from the constants of Table 4, where the distortion constants for most of the excited states have abnormal magnitudes. By combining our experimental results with our *ab initio* calculations on the low-lying electronic states of TaN we have been able to draw some useful conclusions about the ground state and a few low-lying excited states. The observation of two intercombination transitions between the singlet and triplet states of TaN has provided a conclusive electronic assignment of the ground state. The experimental equilibrium constant of $B_e = 0.458\,521(48)$ cm^{-1} for the ground state provides an equilibrium bond length of $R_e = 1.683\,099\,9(88)$ Å for the $X^1\Sigma^+$ state. This assignment is well supported by the *ab initio* calculations, which also predict a $^1\Sigma^+$ ground state with a bond length of $R_e = 1.706$ Å. This value also compares well with the value of $R_e = 1.690$ Å obtained using density functional calculations by Zhou and Andrews (*15*) in their laser ablation study of TaN. It is somewhat surprising considering the extensive interactions among the excited states that no lower state vibrational interval could be obtained from our spectra, indicating that all of the observed transitions (or subbands) are highly diagonal. This has been the case for the observed singlet as well as triplet transitions.

Our analysis locates, the $a^3\Delta_1$ state at 2827 cm^{-1} above the ground state with $B_e = 0.453\,324\,2(43)$ cm^{-1}, which provides an experimental bond length of $R_e = 1.691\,484\,6(80)$ Å. This also compares reasonably well with the *ab initio* values of $T_0 = 4276\,cm^{-1}$ and $R_e = 1.714$ Å. Note that our *ab initio* calculations do not include the effects of spin orbit coupling. The $a^3\Delta$ term state is regular and if spin–orbit coupling is included then the $a^3\Delta_1$ spin component will be shifted by at least 1000 cm^{-1} to lower energy (*30*), in better agreement with the observations.

Even after the analysis of so many new bands, the assignment of the higher-lying excited electronic states remains very difficult. This is because of the Hund's case (c) behavior of these states. As predicted by the *ab initio* calculations there are 11 terms and some 27 spin components between about 18 000 and 25 000 cm^{-1}. If strong spin orbit coupling is introduced (ζ_{5d} for Ta is 1699 cm^{-1} (*30*)) then many of the terms become heavily mixed and only Ω remains a good quantum number. A particularly confusing aspect of the analysis is the vibrational assignment of the bands. Near the 0–0 bands of group I should lie the 1–1 bands of group II, but this is not the case. Some of the bands are missing because they are too heavily perturbed to be analyzed. Other bands are evidently shifted by electronic interactions that seem to preserve the diagonal character of the vibrational bands.

CONCLUSION

The emission spectrum of TaN has been investigated in the region 3000–35 000 cm^{-1} using a Fourier transform spectrometer. Many new bands were observed in addition to the previously known bands (*13*) and have been classified into four groups. A $^1\Sigma^+$ state has been assigned as the ground state of TaN based on our analysis and supported by our *ab initio* calculations. Also, $a^3\Delta_1$ state at 2827 cm^{-1} above the ground state has been identified as the first excited state of TaN. This assignment is also supported by our *ab initio* calculations. The higher wavenumber region has many singlet and triplet states that strongly interact with each other. Most of the excited states are thus affected by global and local perturbations. The observed excited states have been labeled with their Ω-values, and in some cases even these Ω values are not secure.

ACKNOWLEDGMENTS

We thank M. Dulick, C. Plymate, and D. Branston of the National Solar Observatory for assistance in obtaining the spectra. The Kitt Peak National Observatory and the National Solar Observatory are operated by the Association of Universities for Research in Astronomy, Inc., under contract with the National Science Foundation. The research described here was supported by funding from the NASA laboratory astrophysics program. Some support was also provided by the Natural Sciences and Engineering Research Council of Canada. J.L. thanks the Fonds National de la Recherche Scientifique de Belgique for financial support. We thank T. Dunn for sending us the relevant chapters on TaN from the Ph.D. thesis of J. K. Bates.

REFERENCES

1. F. A. Cotton, G. Wilkinson, C. A. Murillo, and M. Bochmann, "Advanced Inorganic Chemistry, A Comprehensive Text," 6th ed. Wiley, New York, 1999.
2. M. Grunze, *in* "The Chemical Physics of Solid Surfaces and Heterogeneous Catalysis" (D. A. King and D. P. Woodruff, Eds.), Vol. 4, p. 143. Elsevier, New York, 1982.
3. F. Gassner, E. Dinjus, and W. Leitner, *Organometallics* **15,** 2078–2082 (1996).
4. M. A. Casado, J. J. Perez-Torrente, M. A. Ciriano, L. A. Oro, A. Orejon, and C. Claver, *Organometallics* **18,** 3035–3044 (1999).
5. R. W. Boyle, J. Lautenbach, and W. H. Weinberg, *Ind. Eng. Chem. Res.* **35,** 2986–2992 (1996).

6. C. W. Bauschlicher, Jr., S. P. Walch, and S. R. Langhoff, "Quantum Chemistry: The Challenge of Transition Metals and Coordination Chemistry" (A. Veillard, Ed.), NATO ASI Ser. C. Reidel, Dordrecht, 1986.
7. D. L. Lambert and R. E. S. Clegg, *Mon. Not. R. Astron. Soc.* **191,** 367–389 (1980).
8. O. Engvold, H. Wöhl, and J. W. Brault, *Astron. Astrophys. Suppl. Ser.* **42,** 209–213 (1980).
9. B. Lindgren and G. Olofsson, *Astron. Astrophys.* **84,** 300–303 (1980).
10. R. S. Ram, P. F. Bernath, and L. Wallace, Astrophys. *J. Suppl. Ser.* **107,** 443–449 (1996).
11. A. J. Merer, *Annu. Rev. Phys. Chem.* **40,** 407–438 (1989).
12. P. F. Bernath, "Transition Metal Hydrides," Advances in Metal and Semiconductor Clusters (M. Duncan, Ed.), Vol. 5, Elsevier, Amsterdam, 2001.
13. J. K. Bates, "Optical Emission Spectra of Diatomic Metal Nitrides," Ph.D. thesis. University of Michigan, 1975; T. M. Dunn, personal communication.
14. J. K. Bates and D. M. Gruen, *J. Chem. Phys.* **70,** 4428–4429 (1979).
15. M. Zhou and L. Andrews, *J. Phys. Chem.* **102,** 9061–9071 (1998).
16. R. S. Ram, J. Liévin, and P. F. Bernath, *J. Chem. Phys.* **109,** 6329–6337 (1998).
17. R. S. Ram, J. Liévin, and P. F. Bernath, *J. Mol. Spectrosc.* **197,** 133–146 (1999).
18. R. S. Ram, J. Liévin, and P. F. Bernath, *J. Chem. Phys.* **111,** 3449–3456 (1999).
19. R. S. Ram, J. Liévin, G. Li, T. Hirao, and P. F. Bernath, *Chem. Phys. Lett.* **343,** 437–445 (2001).
20. R. S. Ram, A. G. Adam, A. Tsouli, J. Liévin, and P. F. Bernath, *J. Mol. Spectrosc.* **202,** 116–130 (2000).
21. R. S. Ram, A. G. Adam, W. Sha, A. Tsouli, J. Liévin, and P. F. Bernath, *J. Chem. Phys.* **114,** 3977–3987 (2001).
22. H.-J. Werner and P. J. Knowles, J. Chem. Phys. **82,** 5053–5063 (1985); P. J. Knowles and H.-J. Werner, *Chem. Phys. Lett.* **115,** 259–267 (1985).
23. H.-J. Werner and P. J. Knowles, *J. Chem. Phys.* **89,** 5803–5814 (1988); P. J. Knowles and H.-J. Werner, *Chem. Phys. Lett.* **145,** 514–522 (1988).
24. S. R. Langhoff and E. R. Davidson, *Int. J. Quantum Chem.***8,** 61–72 (1974).
25. D. Andrae, U. Häußermann, M. Dolg, H. Stoll, and H. Preuss, *Theor. Chim. Acta* **77,** 123–141 (1990).
26. A. Bergner, M. Dolg, W. Küechle, H. Stoll, and H. Preuß, *Mol. Phys.* **80,** 1431–1441 (1993).
27. H.-J. Werner and P. J. Knowles, with contributions from R. D. Amos, A. Bernhardsson, A. Berning, P. Celani, D. L. Cooper, M. J. O. Deegan, A. J. Dobbyn, F. Eckert, C. Hampel, G. Hetzer, T. Korona, R. Lindh, A. W. Lloyd, S. J. McNicholas, F. R. Manby, W. Meyer, M. E. Mura, A. Nicklass, P. Palmieri, R. Pitzer, G. Rauhut, M. Schütz, H. Stoll, A. J. Stone, R. Tarroni, and T. Thorsteinsson, MOLPRO, Version 2000.1.
28. G. Schaftenaar and J. H. Noordik, *J. Comput.-Aided Mol. Design* **14,** 123–134 (2000).
29. B. A. Palmer and R. Engleman, "Atlas of the Thorium Spectrum." Los Alamos National Laboratory, Los Alamos, NM, 1983.
30. H. Lefebvre-Brion and R.W. Field, "Perturbations in the Spectra of Diatomic Molecules." Academic Press, San Diego, 1986.